Novel Method for Rapid Monitoring of Lipid Oxidation by FTIR Spectroscopy Using Disposable IR Cards

Ted A. Russin, Frederick R. van de Voort*, and Jacqueline Sedman

McGill IR Group, Department of Food Science and Agricultural Chemistry, Macdonald Campus of McGill University, Sainte-Anne-de-Bellevue, Québec, Canada H9X 3V9

ABSTRACT: A new FTIR approach was investigated for assessing edible oil oxidative stability with the use of polymer IR (PIR) cards as sample holders. This approach allows oil oxidation to be monitored at moderate temperatures owing to the fairly rapid rate at which unsaturated oils oxidize on the PIR cards. To assess the FTIR/PIR card method, pure TAG—triolein, trilinolein, and trilinolenin—were loaded onto cards and placed in a chamber where warm air (55°C) flowed over them continuously to facilitate oxidation. At periodic intervals, individual cards were removed and their FTIR spectra scanned, after which they were replaced in the aeration chamber. All spectra were normalized to compensate for variations in PIR card path lengths or oil loadings, and for each card the initial spectrum recorded ($t = 0$) was subtracted from all subsequent spectra taken over time to produce differential spectra. With the use of a peak-find algorithm, the absorbance minimum in the *cis* region (3017–3000 cm^{-1}) and the absorbance maxima in the hydroperoxide (3550–3200 cm^{-1}), isolated *trans* (977–957 cm^{-1}), and conjugated *trans* regions (995–983 cm^{-1}) were measured in the differential spectra and plotted as a function of time. For all three TAG, the loss of *cis* double bonds was linearly related to the development of hydroperoxides and isolated *trans* bonds for much of the oxidation process, whereas for the polyunsaturated TAG a similar relationship also existed for conjugated *trans* species. Based on an experimentally determined hydroperoxide (ROOH) absorbance slope factor (0.06 mAbs/PV), ROOH absorbance changes were converted to PV, allowing direct PV monitoring as a function of time using the PIR cards. Trilinolenin, trilinolein, and triolein attained a PV of 100 mequiv/kg oil after 43, 98, and 2889 min, respectively, their relative reaction rates being similar to ratios published in the literature. The assessment of the FTIR/PIR card method using TAG indicates that it may be a practical and rapid means of oxidizing lipids and tracking their oxidative state in terms of PV so as to provide a measure of their oxidative stability.

Paper no. J10433 in *JAOCS 80,* 635–641 (July, 2003)

KEY WORDS: Autoxidation, edible oils, FTIR spectroscopy, IR polymer cards, monitoring, oxidative stability, triacylglycerols, trilinolein, trilinolenin, triolein.

The autoxidation of polyunsaturated edible oils is of major concern in relation to their stability and the quality of the products in which they are incorporated. Oxidative breakdown of unsaturated FA causes a variety of deleterious changes, affecting both their functional and organoleptic properties (1) and reducing their bioavailability (2). Thus, for purposes of quality control and estimation of shelf life of bulk lipids and lipid-containing products, it is crucial to have a valid measure of the resistance of lipids to oxidation (3), especially under conventional storage conditions (4,5). For practical reasons, oxidative stability assessment is usually carried out under conditions of accelerated oxidation, commonly achieved through the use of elevated temperatures (Table 1). In this regard, the two most commonly used tests, the Active Oxygen Method (AOM) and the Oil Stability Index (OSI), have been criticized for using excessively high temperatures at which the reaction pathways deviate significantly from those taking place at room temperature (5). In contrast, the Oven Storage Test (OST), commonly known as the Schaal Oven Test, uses a relatively low temperature (60°C) but, as a result, is a very slow test, typically lasting 4–8 d (7). Thus, none of the methods listed in Table 1, nor any of the other methods available for evaluating oil stability, meets the general need for a practical, rapid method representative of oxidative reactions occurring in oils stored under ambient conditions (8,9).

FTIR spectroscopy is a powerful instrumental tool for both qualitative and quantitative analysis of edible oils owing to the substantial functional group information contained within the IR spectrum (10). FTIR spectroscopy has been used to study oil oxidation either by sequentially recording the spectra of samples taken over time from oils under oxidative stress (11–13) or by continuously monitoring spectral changes in oils spread on the surface of a heated, attenuated total reflectance (ATR) crystal, where oxidation occurs fairly rapidly owing to the high surface area of the oil exposed to air (11,14). The ATR approach has the advantage of allowing the spectral changes associated with oil oxidation to be monitored dynamically and within a reasonable time frame (typically 24–48 h). However, this technique, although useful for research purposes, is impractical for routine quality control monitoring of oil oxidation as it requires that the spectrometer be dedicated to the analysis of a single sample for the duration of the monitoring period.

This paper presents a new FTIR approach for measuring oxidative stability through the use of disposable polymer IR (PIR) cards. This approach provides a means of overcoming the single-sample limitation of the ATR technique and allows oxidative changes to be monitored at more moderate temperatures. In this study, the PIR oxidation/analysis system was evaluated

*To whom correspondence should be addressed at the McGill IR Group, Department of Food Science and Agricultural Chemistry, Macdonald Campus of McGill University, 21,111 Lakeshore Rd., Sainte-Anne-de-Bellevue, Québec, Canada H9X 3V9. E-mail: vandevoort@macdonald.mcgill.ca

Copyright © 2003 by AOCS Press

TABLE 1
AOCS Methods Commonly Used for Assessing Oil Oxidative Stability

Method	AOCS method[a]	Test conditions	Strengths	Weaknesses
Oven Storage Test (OST)	Recommended Practice Cg 5–97	60°C, end point based on sensory evaluation, PV, or GC volatile compounds	Moderate temperature, simple method	Very slow, lacks precision
Active Oxygen Method (AOM)	Official Method Cd 12-57 (declared obsolete in 1993)	97.8°C, end point defined as PV = 100 mequiv/kg oil	Very fast, inexpensive	High temperature, unrepresentative of storage conditions
Oil Stability Index (OSI)	Official Method Cd 12b-92	100–140°C, end point based on conductivity due to volatile short-chain organic acids	Very fast, automated	High temperature, unrepresentative of storage conditions

[a]Reference 6.

using pure TAG rather than more complex lipid systems so as to simplify the interpretation of the spectral data obtained.

MATERIALS AND METHODS

Materials. Triolein ($^3C_{18:1}$) and trilinolein ($^3C_{18:2}$) were obtained from Sigma-Aldrich (St. Louis, MO), and trilinolenin ($^3C_{18:3}$) was obtained from Nu-Chek-Prep (Elysian, MN); all had a purity of ≥99%. Sunflower oil was purchased from a local supermarket.

PIR cards. For this work, samples were applied onto Thermo Nicolet (Madison, WI) dual-aperture Type 2 ST-IR™ PIR cards (Scheme 1). The cards fit into a standard FTIR cell mount (5.0 × 10.8 cm) and consist of a microporous polytetrafluoroethylene (PTFE) polymer sandwiched between two cardboard layers having two 1.90-cm apertures. The polymer is transparent to mid-IR radiation except in two spectral regions (1270–1100 and 660–460 cm^{-1}) where PTFE absorbs.

Sample preparation/oxidation. $^3C_{18:1}$, $^3C_{18:2}$, and $^3C_{18:3}$ were used as model systems to study lipid oxidation on the PIR cards. Cards were loaded by applying three drops (~0.075 g) of neat TAG onto both sides of the aperture using a disposable 3.5-mL transfer pipette. The sample was spread over the entire aperture using a cotton swab to ensure a uniform distribution, and then the aperture was blotted with a tissue to remove any excess sample. Each TAG was loaded onto the aperture pairs of two cards (four replicates of each TAG), and the cards were placed into a Plexiglas aeration chamber installed in a laboratory oven (Lab-Line Instruments, Inc., Melrose Park, IL). The aeration chamber was connected to a vacuum line to aspirate warm oven air past the cards at a controlled rate and to exhaust any volatiles produced by the oxidation process, thereby eliminating their possible prooxidative effects. The chamber exit air temperature was monitored using a thermocouple and was maintained at 55 ± 4°C. Each card was periodically removed from the chamber, the time recorded, and the spectrum of each of its apertures scanned, a process that takes about 2 min. In a separate series of experiments, 200 μL of neat TAG was applied onto the surface of a heated horizontal ATR (HATR) accessory equipped with a 45° ZnSe crystal (Thermo Nicolet) maintained at 57 ± 0.5°C, and spectra were collected at preprogrammed intervals. All ATR spectra were corrected to compensate for changes in effective path length as a function of wavelength to produce conventional constant-path-length spectra.

Instrumentation/data collection. The PIR cards were scanned using a Bomem FTIR spectrometer (MB Series; ABB Bomem, Inc., Québec, Canada) run under Bomem-Grams/386 software (Thermo Galactic, Salem, NH), and the ATR experiments were run on a 5DXC FTIR spectrometer under OMNIC software (Thermo Nicolet). Both instruments were equipped with deuterated triglycine sulfate detectors and purged with dry, CO_2-free air supplied by a Balston dryer (Balston, Lexington, MA). The PIR card spectra were collected by co-addition of 16 scans and ratioed against an open-beam background spectrum, whereas the ATR spectra were acquired using 512 scans and ratioed against the spectrum of the clean crystal. All spectra were collected at a resolution of 4 cm^{-1}.

Data processing. A reference absorbance spectrum of each TAG was taken at $t = 0$ for both the card and the ATR experiments. An automated data processing routine was developed (i) to correct for offset/tilt of the spectral baseline, (ii) to normalize each spectrum to unit height of the maximum of the ν(CH)

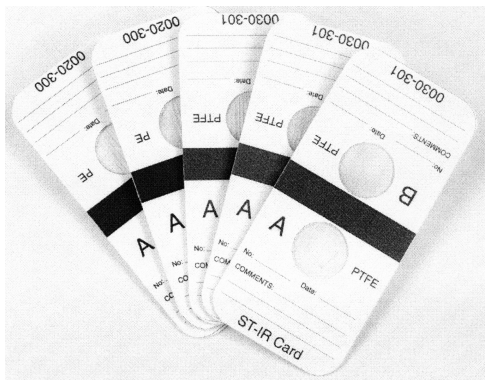

SCHEME 1

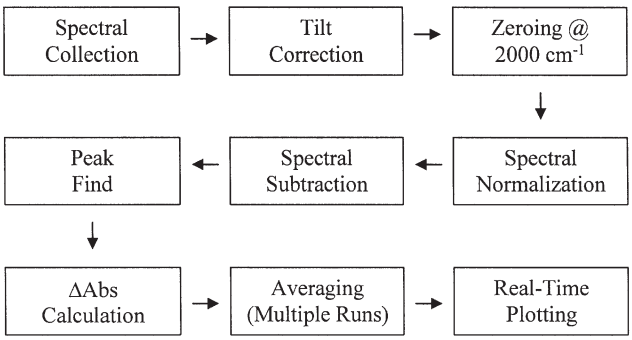

SCHEME 2

absorption band at ~2854 cm^{-1}, the absorption maximum being located within the range of 2865–2840 cm^{-1} by a peak-find algorithm, (iii) to subtract the $t = 0$ spectrum from all subsequent spectra to produce differential spectra, (iv) to find peak maxima or minima within selected spectral ranges, and (v) to output the peak locations and the corresponding absorbance values.

Bulk oxidation/PV calibration. Fresh sunflower oil (100 mL) was oxidized by passing oven-warmed air over the vigorously stirred oil, maintained at 60°C, for 6 d. The oxidized oil was used to prepare a set of standards, ranging from 4.5 to 80% oxidized oil, by gravimetrically diluting it with aliquots of fresh sunflower oil. These standards as well as the oxidized oil and the fresh oil were loaded onto PIR cards in the same manner as the TAG to acquire their FTIR spectra. After spectral normalization and subtraction of the spectrum of the fresh oil, the location and absorbance value of the ROOH absorption maximum in the spectrum of each standard were measured. Seven of the standards were also analyzed for PV by the FTIR/triphenylphosphine (TPP) method developed by Ma *et al.* (15), which uses a 190-μm KCl transmission cell. These standards, in which the percentage of oxidized oil ranged from 4.5 to 20%, were further diluted 60-fold with fresh sunflower oil to bring the hydroperoxide levels into the analytical range of the method (0–15 PV) and were analyzed in duplicate. The ROOH absorbance data obtained from the normalized PIR card spectra of the standards were regressed against the PV data (adjusted by the dilution factor) to obtain a PV absorbance slope factor (ASF), expressed as mAbs/PV, for card spectra normalized to unit height of the ~2854-cm^{-1} band. The ASF is representative of the product of the extinction coefficient and the path length.

RESULTS AND DISCUSSION

Analytical concepts and issues. Ideally, a method for assessing oxidative stability of oils should meet three basic criteria: (i) oxidation takes place efficiently at low to moderate temperatures (40–60°C), (ii) significant and measurable oxidative changes occur within hours, and (iii) a simple quantitative measurement is available to provide an estimate of the comparative stabilities of oils. Our previous work (11,14) suggested that these criteria potentially could be met through the application of FTIR spectroscopy to dynamically monitor oil oxidation, but the method developed was impractical for routine use since only a single sample could be monitored per test and each such test would monopolize the FTIR spectrometer for an extended period of time. In subsequent work, in which 3M-PIR cards (St. Paul, MN; now discontinued) were used for the quantitative analysis of PV and *trans* content of edible oils (16,17), it was noted that polyunsaturated oils loaded onto these cards oxidized quite rapidly. This observation led us to consider the substitution of microporous PIR cards for the ATR accessory used in our earlier work, as it would facilitate the analysis of multiple samples as well as free the spectrometer for other uses.

The potential use of PIR cards in this capacity required that a number of issues be addressed. First, to compare spectral data from different cards, one must be able to compensate for the variability in polymer film thickness and sample loading by normalizing all spectra to unit height of an appropriate absorption band, as discussed previously in relation to the discontinued 3M cards (16,17). Second, with the Thermo Nicolet PIR cards used in this study, there is the additional complication of ongoing sample diffusion because, unlike the 3M cards, these PIR cards do not incorporate a nonporous barrier around the perimeter of the aperture to limit sample spreading to a defined area. Thus, comparison of the spectra recorded from a single card over time, as well as those recorded from different cards, requires spectral normalization. Third, the use of a peak-find algorithm was necessary to determine normalization factors accurately and to measure absorbance changes associated with oxidative changes, owing to band shifts occurring as a result of oxidation or other factors. These various issues, as well as the need to automate the analysis of the large amounts of spectral data generated during the oxidation experiments, were addressed by writing a data processing routine incorporating the steps outlined in the flowchart presented in Scheme 2.

TABLE 2
Literature Peak Locations for Oxidation Indicator Bands, Spectral Ranges Searched to Find the Spectral Maximum or Minimum (*cis*), and Baseline Points Employed to Which ΔAbs Values[a] Were Referenced

Absorption band	Literature (cm^{-1})	Peak-find range (cm^{-1})	Baseline 1 (cm^{-1})	Baseline 2 (cm^{-1})
ROOH	3444[b]	3550–3200	3649.0	3649.0
cis	3011–3005[c]	3017–3000	3049.2	3049.2
Conjugated *trans*	987[b]	995–983	1004.8	929.6
Isolated *trans*	969[b]	977–957	1004.8	929.6

[a]ΔAbs: difference in absorbance data.
[b]Reference 11.
[c]Reference 18; position shifts from 3011 cm^{-1} for $^3C_{18:3}$ to 3009 cm^{-1} for $^3C_{18:2}$ and 3005 cm^{-1} for $^3C_{18:1}$.

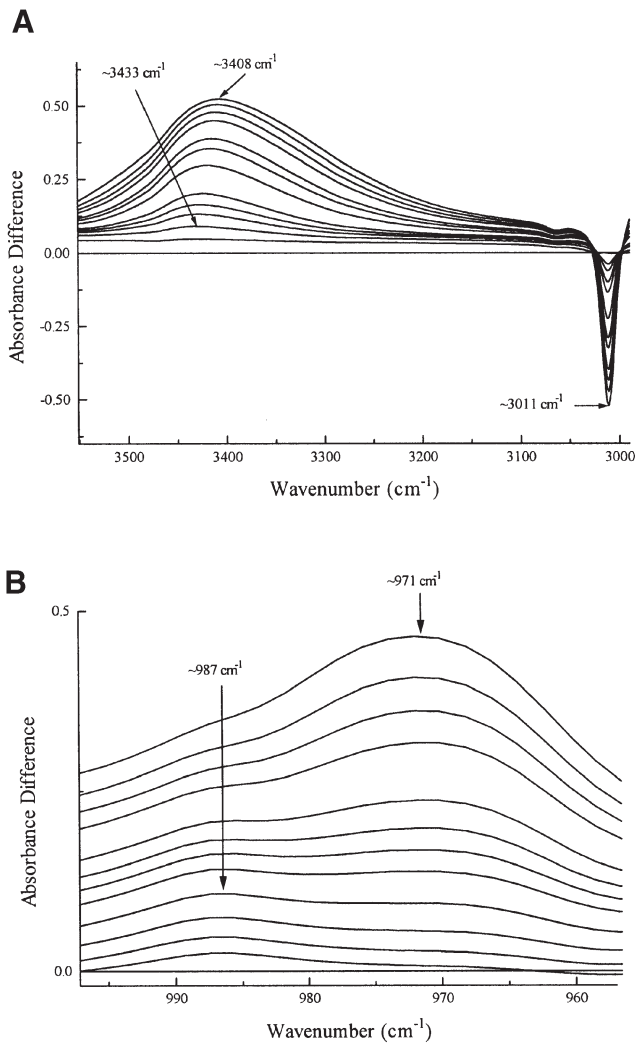

FIG. 1. Time series differential spectra of trilinolenin ($^3C_{18:3}$): (A) ROOH (~3433 to ~3408 cm^{-1}) and *cis* (~3011 cm^{-1}) absorptions, illustrating hydroperoxide formation and progressive shifting of the ROOH band with concomitant loss of *cis* double bonds; (B) *trans* region, showing the initial formation of conjugated *trans* species (~987 cm^{-1}) followed by the formation of species containing isolated *trans* bonds (~971 cm^{-1}).

PIR card differential spectra. For this work, pure triolein, trilinolein, and trilinolenin were selected as model systems since $C_{18:1c}$, $C_{18:2c}$, and $C_{18:3c}$ are common constituents of edible oil TAG. The raw spectral data obtained from the cards were processed in the sequence outlined in Scheme 2 to produce differential spectra and extract both peak location (cm^{-1}) and absorbance (ΔAbs) data for the absorption maxima (minimum for *cis*) within the spectral regions outlined in Table 2, the ΔAbs data subsequently being plotted as a function of time to generate "real-time oxidation plots." Figure 1 presents a typical time series of differential spectra for $^3C_{18:3}$ undergoing oxidation, focusing on selected regions in which obvious spectral changes take place as oxidation proceeds. In these differential spectra, produced by subtraction of the $t = 0$ spectrum, all the invariant spectral features associated with the oil are removed, leaving only the spectral changes associated with the oxidation process. Figure 1A illustrates the decrease of the *cis* double bond absorption (~3011 cm^{-1}) over time with the concomitant formation of hydroperoxides (absorption initially at ~3433 cm^{-1} and gradually shifting to ~3408 cm^{-1}), whereas Figure 1B illustrates concurrent changes in the *trans* region, showing the initial formation of conjugated *trans* species (~987 cm^{-1}) followed by the appearance of isolated *trans* absorptions (~971 cm^{-1}). Time series spectra of both $^3C_{18:2}$ and $^3C_{18:1}$ were similar in form, the exception being the absence of conjugated *trans* absorptions in the case of $^3C_{18:1}$ as oleic acid has only one double bond. However, the ΔAbs magnitudes of the oxidation indicator bands differed markedly among the three TAG.

Of particular interest in Figure 1 is the very large shift (~25 cm^{-1}) over time in the position of the ROOH band toward lower wavenumbers, well away from the literature value of 3444 cm^{-1} (11). Subsequently, much later in the oxidation process, there was a shift back toward higher wavenumbers, resulting from the breakdown of hydroperoxides to alcohols, which absorb at ~3544 cm^{-1} (11). The ROOH band shifts were common to all the TAG and also were observed when the TAG were oxidized on a heated ATR crystal at 57°C. In contrast, only minimal (1–2 cm^{-1}) shifts of the *cis*, conjugated *trans*, and isolated *trans* bands occurred over time. Guillén and Cabo (12) also reported a shift of the ROOH band toward lower wavenumbers as oils underwent oxidation at 60°C, but to a somewhat lesser extent. Similar band shifts observed in the FTIR spectra of alcohols at high concentrations in *n*-decane have been attributed to cluster formation (19); thus, it may be postulated that the ROOH band shift is due to extensive intermolecular hydrogen bonding of hydroperoxides resulting from their accumulation at high concentrations in the card matrix at the moderate temperatures used. In experiments performed to investigate this further, sunflower oil was oxidized at 60°C for 6 d and then serially diluted with fresh sunflower oil to produce seven standards ranging from 10 to 100% oxidized oil. The PIR card spectra of these standards showed a shift of the ROOH peak maximum to lower wavenumbers concurrent with the increase in the intensity of this peak as the proportion of oxidized oil in the samples increased, confirming the concentration dependence of the position of the ROOH band (Fig. 2). Additional standards were also analyzed for PV in a transmission cell by the FTIR/TPP method (15) to determine an ASF for the ROOH band in the normalized card spectra, allowing ROOH absorbance values to be converted to PV. Based on the value of 0.06 mAbs/PV obtained, it became apparent that unusually high PV (1000–7000 mequiv/kg oil, depending on the TAG) are reached during oxidation of the TAG on the PIR cards, which could account for the large ROOH band shifts observed.

The pronounced shift of the ROOH absorption maximum over time made it impossible to track the changes in this band properly by measurements at a fixed peak location, making it imperative to incorporate a peak-find routine in the analysis of the spectral data (Scheme 2). This routine also compensated for the differences in the position of the *cis* band in the spectra of the three TAG (Table 2) and for the slight variability (3–4 cm^{-1}) in the positions at which the conjugated and isolated

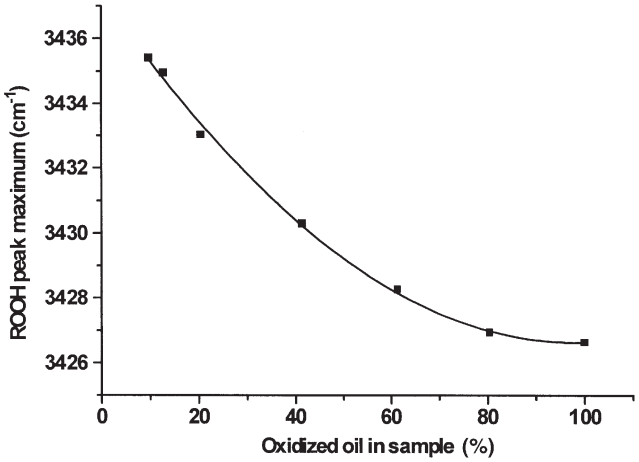

FIG. 2. Plot of position of absorption maximum of ROOH peak in polymer IR (PIR) card spectra of standards prepared by serial dilution of oxidized sunflower oil with fresh sunflower oil vs. the percentage of oxidized oil in the standards.

trans absorptions appear as oxidation proceeds. In this regard, the effects of variability in peak locations are likely to be magnified when mixed glycerides, such as real oils, are analyzed.

Real-time oxidation plots. Figure 3 presents "real-time oxidation plots" (ΔAbs vs. time) for the three TAG, illustrating the *cis*, ROOH, isolated *trans*, and conjugated *trans* band absorbance changes measured from the differential spectra using a peak-find routine to compensate for band shifts. For all TAG, there is a loss of *cis* double bonds with a concurrent rise in hydroperoxides and in isolated *trans* and conjugated *trans* species, except in the case of $^3C_{18:1}$, which does not give rise to conjugated *trans* species. For times beyond those presented in Figure 3, the plots generally plateau and then the curves for the ROOH and *trans* absorptions begin to drop. When the plateau in the *cis* plots is reached, the *cis* absorption is no longer discernible in the raw (unsubtracted) spectra, indicating virtually complete depletion of *cis* double bonds. As expected, the general rate of change and magnitude of ΔAbs increase with the number of double bonds in the TAG. Very similar real-time oxidation profiles were obtained when the TAG were oxidized on a heated ATR crystal at 57°C; however, it took approximately twice as long to attain a similar oxidative state in terms of relative absorbance changes. From a practical perspective, this accelerated rate of oxidation represents an important advantage of the PIR card method over the ATR method.

In the card spectra of all three TAG, the loss of *cis* absorbance correlates linearly with the concurrent increase in ROOH absorbance well into the oxidation process, with the isolated *trans* and conjugated *trans* absorbances showing similar correlations in the case of the two polyunsaturated TAG. These correlations remain constant until well into oxidation and then deteriorate fairly abruptly during the advanced stages. Figure 4 presents an overlay plot showing the interrelationships among the four oxidation indicator bands for $^3C_{18:3}$, with Table 3 providing the linear regression data for all three TAG. These data indicate that the parameters measured are closely interrelated; however, because the relationships differ to some extent among the three TAG, it was concluded that only the ROOH absorption, which is an unambiguous measure of oxidation, can serve as a reliable basis for comparison between samples of different composition.

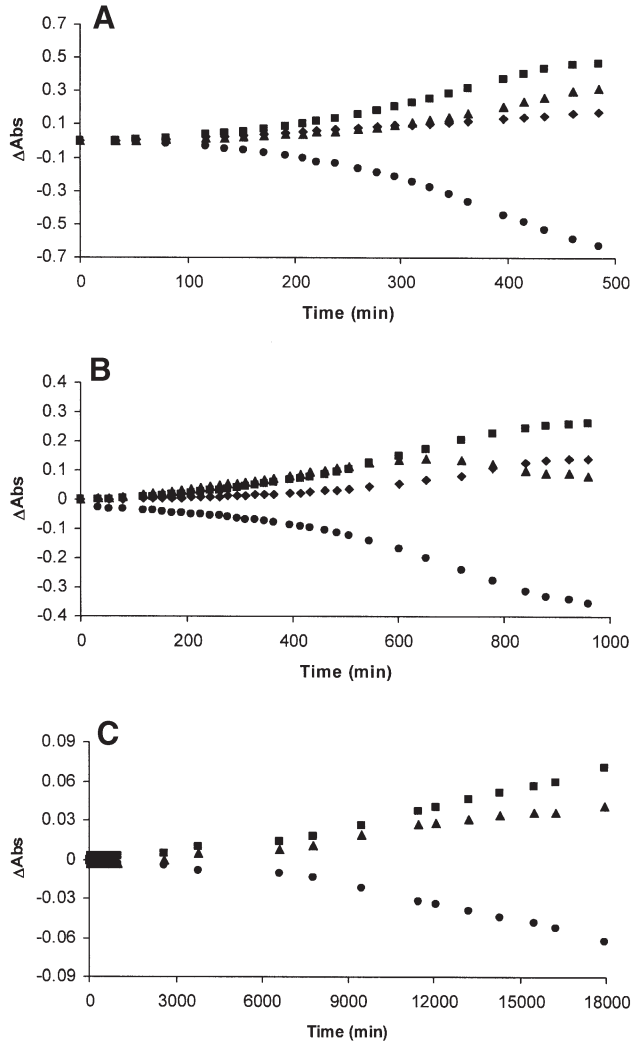

FIG. 3. Real-time oxidation plots (ΔAbs vs. time) obtained for (A) $^3C_{18:3}$, (B) trilinolein ($^3C_{18:2}$), and (C) triolein ($^3C_{18:1}$) using the PIR card method; (●) *cis*, (■) ROOH, (▲) isolated *trans*, and (◆) conjugated *trans*. For abbreviations see Figures 1 and 2.

Conversion of absorbance data to PV data. Although dynamic oxidative profiles can be generated from the PIR card absorbance data, it is desirable to convert these data to PV data so as to obtain a quantitative measure of relative oxidative stability. By dividing the ΔAbs_{ROOH} values by the ASF of the ROOH band, determined to be 0.06 mAbs/PV by a serial dilution of oxidized sunflower oil as described above, PV vs. time plots were generated (Fig. 5). Figure 5, which shows only a small initial portion of the PV oxidative data, provides a basis for comparing the relative stabilities of the TAG through the use of a PV end point. An end point of PV 100, selected to match the end point used in the AOM method, is reached after

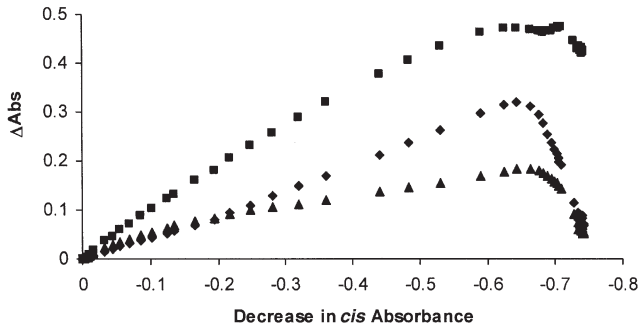

FIG. 4. Overlay plot of ΔAbs for the ROOH (■), isolated *trans* (▲), and conjugated *trans* (◆) absorptions vs. ΔAbs for the decrease in the *cis* absorption in the PIR card spectra of $^3C_{18:3}$, illustrating the correlation between the intensities of the four oxidation indicator bands well into the oxidative process. For abbreviations see Figures 1 and 2.

43, 98, and 2889 min for $^3C_{18:3}$, $^3C_{18:2}$, and $^3C_{18:1}$, respectively. On this basis, $^3C_{18:1}$ is very stable to oxidation, taking about 3 d to reach a PV of 100, whereas $^3C_{18:2}$ and $^3C_{18:3}$ oxidize very rapidly, in a matter of hours. Their relative reaction rates are 1:2.28, close to the ratio of 1:2 that would be predicted on theoretical grounds. The relative reaction rates for $^3C_{18:1}$, $^3C_{18:2}$, and $^3C_{18:3}$ are 1.0:29.5:67.2, in fairly good agreement with the relative rates of oxidation of 1:41:97 reported for ethyl oleate, ethyl linoleate, and ethyl linolenate (20). These results point to the general ability of the PIR card method to provide quantitative data related to the oxidative state of lipids in PV terms, values well understood in the industry.

Based on the study of model lipids, the FTIR/PIR card method appears capable of dynamically monitoring the oxidative stability of edible oils at moderate temperatures, particularly polyunsaturated oils. The model studies show that four oxidation indicator bands can be used to track oxidation and that they are all interrelated. The spectral data can be expressed in terms of PV, thereby providing a measure traditionally used in the assessment of oxidative stability without the need for titrimetric analyses. The advantages of the PIR card method include flexibility, simplicity, speed, and convenience, and the rapid rate of oil oxidation on these cards makes it practical to monitor oxidation at moderate temperatures and facilitates multisample analyses. With the conceptual foundation for the FTIR/PIR card method established, further studies will be carried out with real oils to determine whether the method is suitable for the routine assessment of oxidative stability.

TABLE 3
ROOH, Isolated *trans,* and Conjugated *trans* ΔAbs Values as a Function of *cis* ΔAbs Values for the Three TAG

TAG	ROOH vs. *cis*	Isolated *trans* vs. *cis*	Conjugated *trans* vs. *cis*
$^3C_{18:3}$[a]	–0.961	–0.420	–0.472
$^3C_{18:2}$[b]	–1.238	–0.429	–1.551
$^3C_{18:1}$[c]	–1.150	—[d]	NA

[a]Values are slopes from linear regression performed using the first 15 points (forced through the origin) in the linear portion of the corresponding plot; in all cases, $R^2 > 0.957$. $^3C_{18:3}$, trilinolenin.
[b]Values are slopes from linear regression performed using the first 15 points in the linear portion of the corresponding plot, in all cases, $R^2 > 0.994$. $^3C_{18:2}$, trilinolein.
[c]Value is slope from linear regression performed using the first 47 points in the linear portion of the corresponding plot, $R^2 > 0.996$. $^3C_{18:1}$, triolein.
[d]Nonlinear relationship.

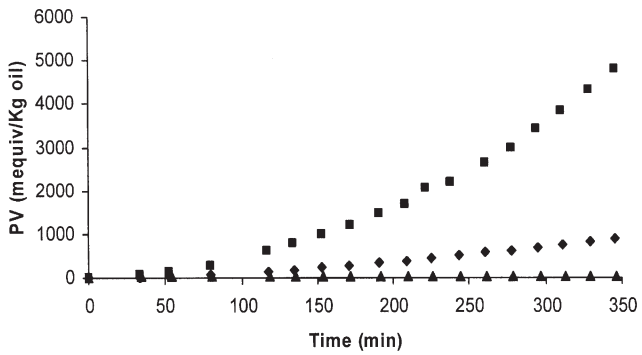

FIG. 5. PV vs. time plot for $^3C_{18:1}$ (▲), $^3C_{18:2}$ (◆), and $^3C_{18:3}$ (■), obtained by converting PIR card ROOH absorbance data to PV data using the absorbance slope factor derived from oxidized sunflower oil serially diluted with fresh sunflower oil. For abbreviations see Figures 1 and 2.

ACKNOWLEDGMENTS

T.A. Russin thanks the Natural Sciences and Engineering Research Council of Canada (NSERC) for a NSERC Postgraduate Scholarship, and the Institute of Food Technologists (IFT), for a graduate fellowship, in support of his graduate studies. The efforts of Mr. Tom Pinchuk are acknowledged for assistance with the programming associated with this work. The authors also thank Thermo Nicolet for supplying the ST-IR PIR cards used in this study.

REFERENCES

1. Smouse, T.H., Significance of Lipid Oxidation to Food Processors, in *Food Lipids and Health*, edited by R.E. McDonald and D.B. Min, Marcel Dekker, New York, 1996, pp. 269–286.
2. Paquette, G., D.B. Kupranycz, and F.R. van de Voort, The Mechanisms of Lipid Autoxidation I. Primary Oxidation Products, *Can. Inst. Food Sci. Technol. J. 18*:112–118 (1985).
3. Gray, J.I., Measurement of Lipid Oxidation: A Review, *J. Am. Oil Chem. Soc. 55*:539–546 (1978).
4. Warner, K. Evaluation of Lipid Quality and Stability, in *Food Lipids and Health*, edited by R.E. McDonald and D.B. Min, Marcel Dekker, New York, 1996, pp. 345–369.
5. Frankel, E.N. *Lipid Oxidation*, The Oily Press, Dundee, Scotland, 1998, pp. 99–114.
6. *Official Methods and Recommended Practices of the American Oil Chemists' Society*, 5th edn., AOCS, Champaign, 1998.
7. Wan, P.J., Accelerated Stability Methods, in *Methods to Assess Quality and Stability of Oils and Fat-Containing Foods*, edited by K. Warner and N.A.M. Eskin, AOCS Press, Champaign, 1995, pp. 179–189.
8. Frankel, E.N., In Search of Better Methods to Evaluate Natural Antioxidants and Oxidative Stability in Food Lipids, *Trends Food Sci. Technol. 4*:220–225 (1993).
9. Hudson, B.J.F., Evaluation of Oxidative Rancidity Techniques, in *Rancidity in Foods*, 2nd edn., edited by J.C. Allen and R.J. Hamilton, Elsevier Applied Science, Essex, England, 1989, pp. 53–65.
10. van de Voort, F.R., J. Sedman, and T. Russin, Lipid Analysis by Vibrational Spectroscopy, *Eur. J. Lipid Sci. Technol. 103*: 815–826 (2001).

11. van de Voort, F.R., A.A. Ismail, J. Sedman, and G. Emo, Monitoring the Oxidation of Edible Oils by Fourier Transform Infrared Spectroscopy, *J. Am. Oil Chem. Soc. 71*:243–253 (1994).
12. Guillén, M.D., and N. Cabo, Usefulness of the Frequency Data of the Fourier Transform Infrared Spectra to Evaluate the Degree of Oxidation of Edible Oils, *J. Agric. Food Chem. 47*:709–719 (1999).
13. Guillén, M.D., and N. Cabo, Some of the Most Significant Changes in the Fourier Transform Infrared Spectra of Edible Oils Under Oxidative Conditions, *J. Sci. Food Agric. 80*:2028–2036 (2000).
14. Sedman, J., A.A. Ismail, A. Nicodemo, S. Kubow, and F.R. van de Voort, Application of FTIR/ATR Differential Spectroscopy for Monitoring Oil Oxidation and Antioxidant Efficiency, in *Natural Antioxidants*, edited by F. Shahidi, AOCS Press, Champaign, 1997, pp. 358–378.
15. Ma, K., F.R. van de Voort, J. Sedman, and A.A. Ismail, Stoichiometric Determination of Hydroperoxides in Fats and Oils by Fourier Transform Infrared Spectroscopy, *J. Am. Oil Chem. Soc. 74*:897–906.
16. Ma, K., F.R. van de Voort, A.A. Ismail, and J. Sedman, Quantitative Determination of Hydroperoxides by Fourier Transform Infrared Spectroscopy with a Disposable Infrared Card, *Ibid. 75*:1095–1101 (1998).
17. Ma, K., F.R. van de Voort, J. Sedman, and A.A. Ismail, *Trans* Fatty Acid Determination in Fats and Margarine by Fourier Transform Infrared Spectroscopy Using a Disposable Infrared Card, *Ibid. 76*:1399–1404 (1999).
18. Ismail, A.A., A. Nicodemo, J. Sedman, F.R. van de Voort, and I.E. Holzbaur, Infrared Spectroscopy of Lipids: Principles and Applications, in *Spectral Properties of Lipids*, edited by R.J. Hamilton and J. Cast, Sheffield Academic Press, Sheffield, England, 1999, pp. 235–269.
19. Forland, G.M., F.O. Libnau, O.M. Kvalheim, and H. Hoiland, Self-Association of Medium-Chain Alcohols in *n*-Decane Solutions, *Appl. Spectrosc. 50*:1264–1272 (1996).
20. Holman, R.T., and O.C. Elmer, The Rates of Oxidation of Unsaturated Fatty Acids and Esters, *J. Am. Oil Chem. Soc. 24*:127–129 (1947).

[Received August 29, 2002; accepted April 18, 2003]